



## Amorphous phase formation by spray forming of alloys [(Fe<sub>0.6</sub>Co<sub>0.4</sub>)<sub>0.75</sub>B<sub>0.2</sub>Si<sub>0.05</sub>]<sub>96</sub>Nb<sub>4</sub> and Fe<sub>66</sub>B<sub>30</sub>Nb<sub>4</sub> modified with Ti

Fausto L. Catto<sup>a</sup>, T. Yonamine<sup>c</sup>, Claudio S. Kiminami<sup>b</sup>, Conrado R.M. Afonso<sup>b</sup>,  
Walter J. Botta<sup>b</sup>, Claudemiro Bolfarini<sup>b,\*</sup>

<sup>a</sup> Programa de Pós-graduação em Ciência e Engenharia de Materiais, Universidade Federal de São Carlos, Rodovia Washington Luiz, km 235, 13565-905, São Carlos, SP, Brazil

<sup>b</sup> Departamento de Engenharia de Materiais, Universidade Federal de São Carlos, Rodovia Washington Luiz, km 235, 13565-905, São Carlos, SP, Brazil

<sup>c</sup> INMETRO, Dimci/Dimat, National Institute of Metrology Standardization and Industrial Quality, RJ, Brazil

### ARTICLE INFO

#### Article history:

Received 23 July 2010

Received in revised form 28 January 2011

Accepted 5 February 2011

Available online 2 March 2011

#### Keywords:

Metallic glasses  
Iron based alloys  
Spray forming  
Amorphous phase

### ABSTRACT

This paper describes results obtained by spray forming three iron-based alloys, namely [(Fe<sub>0.6</sub>Co<sub>0.4</sub>)<sub>0.75</sub>B<sub>0.2</sub>Si<sub>0.05</sub>]<sub>96</sub>Nb<sub>4</sub>, Fe<sub>65</sub>B<sub>30</sub>Nb<sub>4</sub>Ti<sub>1</sub> and Fe<sub>63</sub>B<sub>29</sub>Nb<sub>4</sub>Ti<sub>4</sub>, whose compositions derive from rapid solidification studies, in an attempt to obtain metallic glasses. The [(Fe<sub>0.6</sub>Co<sub>0.4</sub>)<sub>0.75</sub>B<sub>0.2</sub>Si<sub>0.05</sub>]<sub>96</sub>Nb<sub>4</sub> alloy presented higher glass-forming ability and showed a high fraction of amorphous phase formation up to a depth of 4 mm in the deposit. On the other hand, the spray formed deposits of the Fe<sub>65</sub>B<sub>30</sub>Nb<sub>4</sub>Ti<sub>1</sub> and Fe<sub>63</sub>B<sub>29</sub>Nb<sub>4</sub>Ti<sub>4</sub> alloys showed fully crystalline microstructure, despite the fact that the melt spun ribbons were fully amorphous.

© 2011 Elsevier B.V. All rights reserved.

### 1. Introduction

Spray forming (SF) can be classified as a two-stage manufacturing process, where the solidification begins during the flight of the particles, which can be considered a rapid solidification step (10<sup>3</sup>–10<sup>5</sup> K/s), and finishes during the building of the pre-form or deposit, where the remaining liquid droplets solidify under considerable slower cooling rates (10<sup>1</sup>–10<sup>2</sup> K/s) [1]. SF has been successfully applied in processing both commercial and advanced alloys aiming at: the extension of the solid solubility, fine dispersion of second phase particles, low porosity, low segregation level, and finally metastable or even amorphous phases. Nowadays, amorphizable material studies are focused on compositions and processes leading to thicker pieces of bulk metallic glasses (BMGs). For BMG alloys developed in the last decade spray forming may provide the suitable cooling rates associated to a mass production and a near net shape process route.

The [(Fe<sub>0.6</sub>Co<sub>0.4</sub>)<sub>0.75</sub>B<sub>0.2</sub>Si<sub>0.05</sub>]<sub>96</sub>Nb<sub>4</sub> alloy was proposed in 2004 by Inoue et al. [2] and the authors reported super-high yield strength above 4000 MPa. Rods of fully glassy material were produced with 4 mm diameter by the ejection casting method in

a copper mould and the alloy presented  $T_g = 552^\circ\text{C}$ ,  $T_x = 602^\circ\text{C}$  ( $T_x = 50^\circ\text{C}$ ), denoting a very high glass-forming ability with critical cooling rates in the range of 10<sup>1</sup>–10<sup>2</sup> K/s.

Bulk glassy Fe<sub>66</sub>B<sub>30</sub>Nb<sub>4</sub> has been produced by copper mould casting with maximum amorphous thickness up to 1.5–2.0 mm as reported by Stoica et al. [3]. In order to get this result the authors purified the master alloy by fluxing it with B<sub>2</sub>O<sub>3</sub> during a long period of time. Despite its relatively low glass forming ability to be considered a BMG, this is one of the few ternary Fe-based glass former alloys with good mechanical properties, being a very interesting composition for bulk glassy material due to the low cost of the constituent elements. In addition, this alloy presents a high hardness even in the crystalline state, reaching up to 804 HV<sub>0.2</sub>, and can be considered as a candidate for applications where the wear resistance is of importance. Attempts to produce this ternary composition in an amorphous state by spray forming using commercial raw materials led to a maximum amorphous thickness of 0.5 mm, as reported by Bonavina et al. [4]. The affinity between B and Ti suggests a high possibility of titanium boride formation by adding Ti to Fe<sub>66</sub>B<sub>30</sub>Nb<sub>4</sub> alloy, a process that can result in the precipitation of hard borides, still improving the hardness of these compositions.

The main objective of this paper is to evaluate the potential of spray forming to produce metastable or amorphous phases with these iron based alloys that display very distinct abilities for forming metallic glasses, namely [(Fe<sub>0.6</sub>Co<sub>0.4</sub>)<sub>0.75</sub>B<sub>0.2</sub>Si<sub>0.05</sub>]<sub>96</sub>Nb<sub>4</sub> and Fe<sub>66</sub>B<sub>30</sub>Nb<sub>4</sub>. In addition, even considering the possibility to decrease the glass forming ability, the later alloy was modified

\* Corresponding author. Tel.: +55 16 33518534.

E-mail addresses: [fausto.catto@gmail.com](mailto:fausto.catto@gmail.com) (F.L. Catto), [kiminami@ufscar.br](mailto:kiminami@ufscar.br) (C.S. Kiminami), [conrado@ufscar.br](mailto:conrado@ufscar.br) (C.R.M. Afonso), [wjbotta@ufscar.br](mailto:wjbotta@ufscar.br) (W.J. Botta), [cbolfa@ufscar.br](mailto:cbolfa@ufscar.br) (C. Bolfarini).

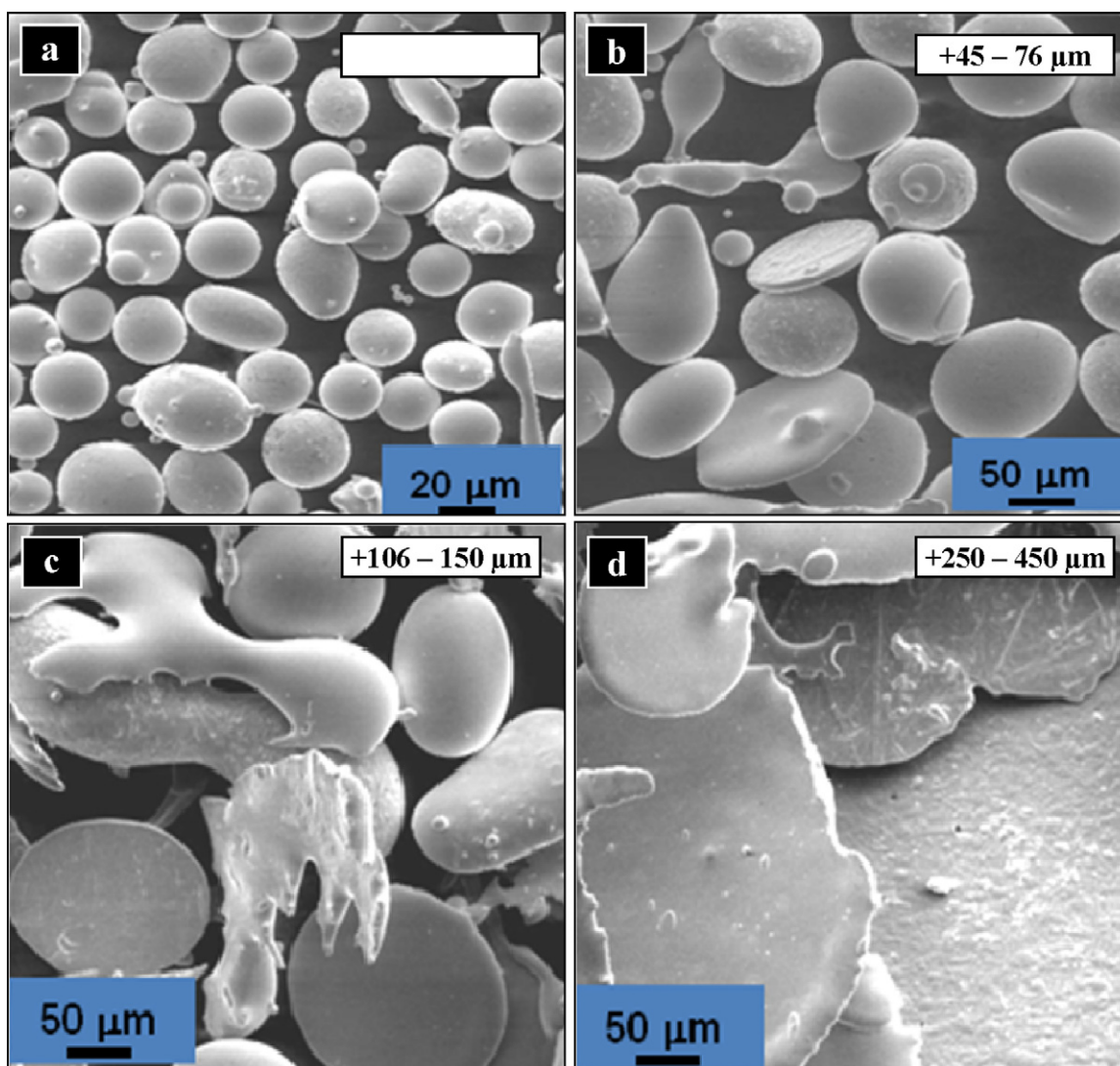


**Fig. 1.** SEM of the overspray powder obtained in experiment SF0. All particles size range (a) +25 to  $-45\ \mu\text{m}$  to (d) +250 to  $-450\ \mu\text{m}$  showed a featureless aspect, indicating amorphous phase formation even for the coarser size ranges and confirming the high glass-forming ability of SF0 composition. Note the deformation of the particles of coarser size ranges and rounded shape of the finer ones.

with the addition of titanium resulting in two distinct alloys:  $\text{Fe}_{65}\text{B}_{30}\text{Nb}_4\text{Ti}_1$  and  $\text{Fe}_{63}\text{B}_{29}\text{Nb}_4\text{Ti}_4$ , as an attempt to obtain deposits with elevated hardness values, aiming at wear resistance applications.

## 2. Methods

Three alloys were processed by melt spinning and spray forming:  $[(\text{Fe}_{0.6}\text{Co}_{0.4})_{0.75}\text{B}_{0.2}\text{Si}_{0.05}]_{96}\text{Nb}_4$ ,  $\text{Fe}_{65}\text{B}_{30}\text{Nb}_4\text{Ti}_1$  and  $\text{Fe}_{63}\text{B}_{29}\text{Nb}_4\text{Ti}_4$  alloys (at%). The molten alloys were poured into a tundish which had a quartz nozzle with a bore of 6 mm diameter in the bottom and then atomized by nitrogen ( $\text{N}_2$ ) with the pressure of 1.0 MPa and flow rate of 3.84 kg/min. A plain carbon steel disk with a diameter of 305 mm was used as a substrate for the atomized droplets in order to form the deposit. The following elements of high purity were used for the alloys preparation: Fe – 99.98%, B – 99.7%, Nb – 99.98% and Ti – 99.99%.

The  $[(\text{Fe}_{0.6}\text{Co}_{0.4})_{0.75}\text{B}_{0.2}\text{Si}_{0.05}]_{96}\text{Nb}_4$  alloy was spray formed at  $1421\ ^\circ\text{C}$  at a G/M (gas to metal ratio) of  $0.94\ \text{m}^3/\text{kg}$  and a flight distance of 425 mm; this experiment is denominated hereinafter as SF0. The overspray powders (materials that were not incorporated in the deposit) were sieved and separated in the size ranges of 20–30, 45–76, 106–150 and 250–450  $\mu\text{m}$ .

The high boron alloys  $\text{Fe}_{63}\text{B}_{29}\text{Nb}_4\text{Ti}_4$  (used in experiment denominated hereinafter as SF1) and  $\text{Fe}_{65}\text{B}_{30}\text{Nb}_4\text{Ti}_1$  (used in experiment denominated hereinafter as SF2) are modifications of a known glass-former alloy,  $\text{Fe}_{66}\text{B}_{30}\text{Nb}_4$ . The processing parameters of SF1 were selected to improve the cooling rate in order to investigate the formation of metastable phases due to its higher Ti content. On the other hand, SF2 was intended to produce a thicker and slowly cooled deposit with higher yield

(efficiency from feedstock to final product conversion) and the presence of stable phases. Flight distances (distance between nozzle to substrate) and pouring temperatures were: 700 mm;  $1600\ ^\circ\text{C}$  for SF1 (cold spray condition, higher cooling rates) and 500 mm;  $1700\ ^\circ\text{C}$  for SF2 (hot spray condition, lower cooling rates), respectively. Melt spun ribbons were produced in order to determine the thermal properties of the alloys studied. For the melt spinning a similar procedure was described in a previous work [1], except for the ejection temperature which was  $1650\ ^\circ\text{C}$ .

The microstructures obtained were characterized by optical microscopy, X-ray diffraction (XRD) in a Siemens D5000 using Cu-K $\alpha$  radiation (with a filter to avoid fluorescence due to iron), Scanning Electron Microscopy (SEM), Philips XL-30, FEG coupled with Energy Dispersive Spectroscopy (EDS), Differential Scanning Calorimetry (DSC), DSC 404 Netzsch, and bulk chemical analysis by Inductively Coupled Plasma Atomic Energy Spectroscopy – ICP-AES and N by thermal conductivity. Porosity was measured using Archimedes method. Vickers hardness measurements were made at low loads ranging from 0.2 and 5 kgf. A number of thirty high load hardness measurements were made onto machined and polished surfaces of SF2 samples using a load of 30 kgf. Test loads were maintained for 20 s.

## 3. Results and discussion

The chemical analysis of the deposits by ICP-AES and EDS/SEM showed that the compositions for SF0 ( $[(\text{Fe}_{0.6}\text{Co}_{0.4})_{0.75}\text{B}_{0.2}\text{Si}_{0.05}]_{96}\text{Nb}_4$ ), SF1 ( $\text{Fe}_{63}\text{B}_{29}\text{Nb}_4\text{Ti}_4$ ) and SF2 ( $\text{Fe}_{65}\text{B}_{30}\text{Nb}_4\text{Ti}_1$ ) experiments are close to the desired nominal compositions, although it was not possible to confirm through

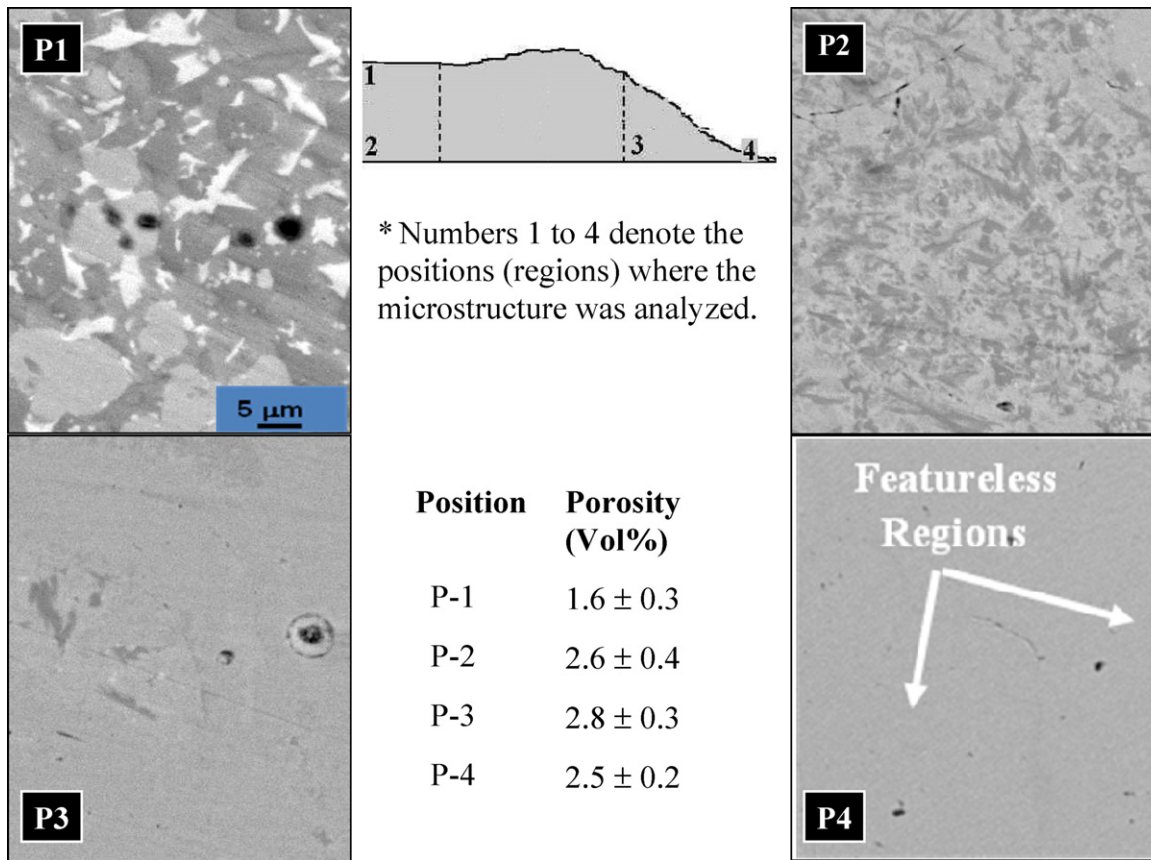


**Fig. 2.** Microstructures in different locations in the SF3 deposit. P1 (16 mm from the bottom): fully crystalline structure with coarse intermetallics; P2 (6 mm from the bottom): partial crystalline structure embedded in an amorphous matrix; P3 (middle of 6 mm thick deposit): partially amorphous structure with some crystalline particles; P4 (middle of 1.5 mm thick deposit): fully amorphous structure.

EDS the quantitative boron composition (at% B) within the alloy's phases.

From the overspray powders of alloy  $[(\text{Fe}_{0.6}\text{Co}_{0.4})_{0.75}\text{B}_{0.2}\text{Si}_{0.05}]_{96}\text{Nb}_4$ , XRD analyses, DSC traces and SEM images (see Fig. 1) showed a high amount of amorphous

phase formation, which attained values over 95% in all the particle size ranges analyzed, as measured by DSC, with a  $\Delta T_x$  of approximately 40 K. These results confirm the high glass-forming ability of the composition used in SFO experiment.

The coarser overspray particles resulted in a deformed or irregular morphology, unlike the spherical shape of the finest size ranges. It is reasonable to assume that these particles hit the wall of the

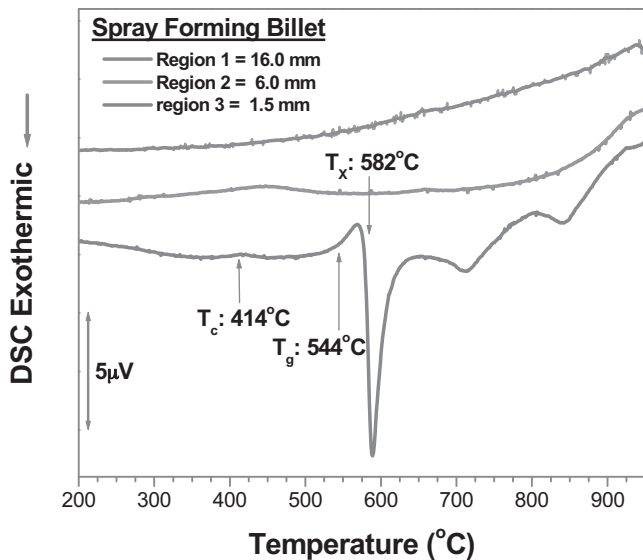


**Fig. 3.** DSC traces for the alloy  $[(\text{Fe}_{0.6}\text{Co}_{0.4})_{0.75}\text{B}_{0.2}\text{Si}_{0.05}]_{96}\text{Nb}_4$ , – central, intermediate and peripheral regions of the deposit: 16.0 (upper trace), 6.0 (intermediate trace) and 1.5 mm (lower trace) thicknesses, respectively.

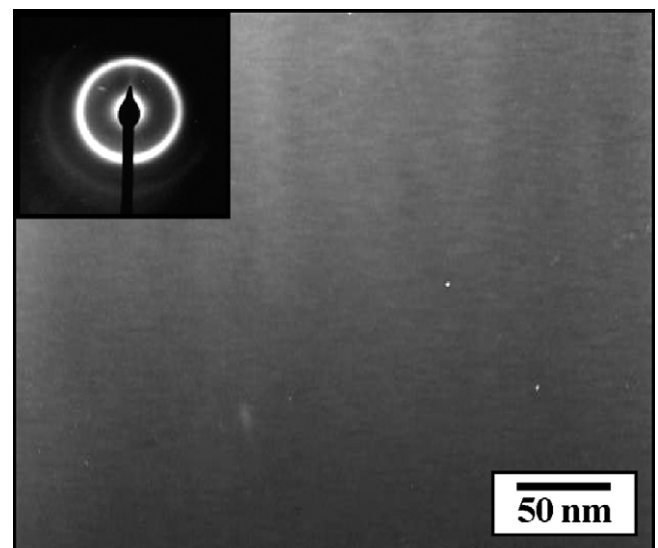


**Fig. 4.** TEM analysis of the thinnest region of the spray formed deposit for alloy  $[(\text{Fe}_{0.6}\text{Co}_{0.4})_{0.75}\text{B}_{0.2}\text{Si}_{0.05}]_{96}\text{Nb}_4$  and SADP showing the amorphous phase formation.

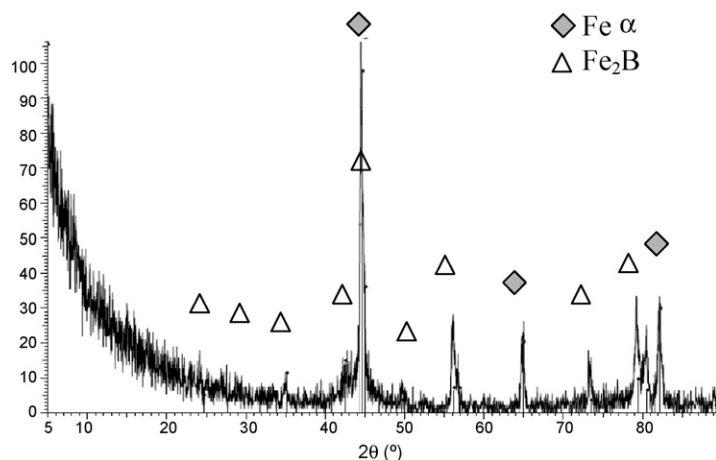


Fig. 5. XRD diffractogram for the unsieved powder of experiment SF2, alloy  $\text{Fe}_{65}\text{B}_{30}\text{Nb}_4\text{Ti}_1$ .

atomization chamber within the supercooled liquid region and were deformed by the impact, providing an extra heat extraction enough to cool down those particles maintaining amorphous structure even in a greater size. These coarse particles, probably, in a similar way would impact the deposit within the supercooled region and contributed significantly to reduce its porosity by filling the space formed between the finest particles that impact the deposit below  $T_g$ . An indication of this effect was suggested by measuring the porosity, as low levels were produced during the deposit build-up, i.e., of about 2.8% (see Fig. 2), whereas the alloys of the SF1 and SF2 experiments presented porosity levels of  $5.0 \pm 0.4$  and  $12.8 \pm 2.4\%$  in volume, respectively, a consequence of the processing parameters and, probably, of the low glass forming ability of these compositions that presented no  $T_g$ , as confirmed by DSC thermal analysis of melt spun ribbons and deposits (not shown in this work). In addition, in comparison with SF1, the porosity obtained for the SF2 experiment was higher since the higher amount of hot material (higher liquid fraction) deposited resulted in a higher fraction of gas entrapment originated from the layers that are closer to the substrate.

As a consequence of this shrinkage mismatch, SF2 deposit presented splitting of layers, and cracks along the diameter, splitting the deposit into two identical halves. SF1 experiment has not presented a macroscopic shrinkage crack between layers, so the gas might have escaped due to the low thickness of the central region of the SF1 deposit (SF1  $\approx 2.5$ – $3$  mm, SF2  $\approx 4$ – $6$  mm) while the material was cooling down. Furthermore, as a consequence of the colder spray condition that led to a higher fraction of solidified droplets

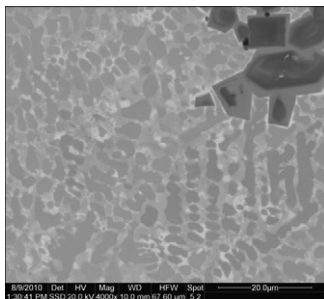


Fig. 6. Microstructure of experiment SF1, alloy  $\text{Fe}_{63}\text{B}_{29}\text{Nb}_4\text{Ti}_4$ . (a) Upper right: coarse  $\text{TiB}_2$  (dark grey) inside  $(\text{Ti,Nb})\text{B}_2$  (bright grey) particles. These coarse borides are heterogeneously distributed across the thickness of the deposit and are identified by X-ray dot mapping (not shown in this work for this composition) and XRD analyses. (b) General view: proeutectic  $\text{Fe}_2\text{B}$  and an eutectic composed of  $\text{Fe}_2\text{B}$ ,  $\alpha$ -Fe and  $\text{FeNb}$  phases.

impacting the substrate to form the deposit, SF1 deposit showed porosity with an irregular morphology (space between solid particles), whereas SF2 deposit produced by hotter condition showed porosity with a round morphology (gas entrapment) due to higher fraction of liquid reaching the deposit during its formation. This effect is well known in spray forming and reported several times in the literature [1,5].

The high glass-forming ability of the composition used in experiment SF0 led to the formation of a high percentage in volume fraction of amorphous phase reaching up to 4 mm thickness in the deposit, a value similar to that obtained for this alloy by copper mould casting, as reported by Inoue et al. [2]. The thicker central regions of the deposit, however, presented crystalline phases and absence of amorphous phase, indicating the inability of this iron-based alloy to maintain the amorphous state observed in the incoming droplets, see Figs. 1 and 2, due to the reheating process promoted by the incoming material as deposition progresses. As it is possible to observe in Fig. 3, a large supercooled liquid range

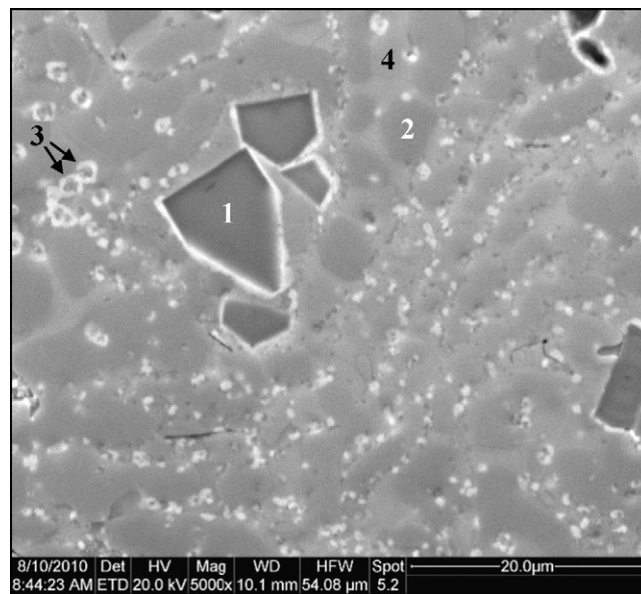


Fig. 7. Microstructure of experiment SF2, alloy  $\text{Fe}_{65}\text{B}_{30}\text{Nb}_4\text{Ti}_1$ . Point 1: coarse  $(\text{Ti,Nb})\text{B}_2$  (faceted dark grey particles). These coarse borides are heterogeneously distributed across the thickness of the deposit and scarce to be observed. Point 2: proeutectic  $\text{Fe}_2\text{B}$ . Point 3: fine precipitation of a second phase in solid state (white particles, niobium, titanium-containing borides, as shown in Figs. 8 and 10). Point 4:  $\alpha$ -Fe.

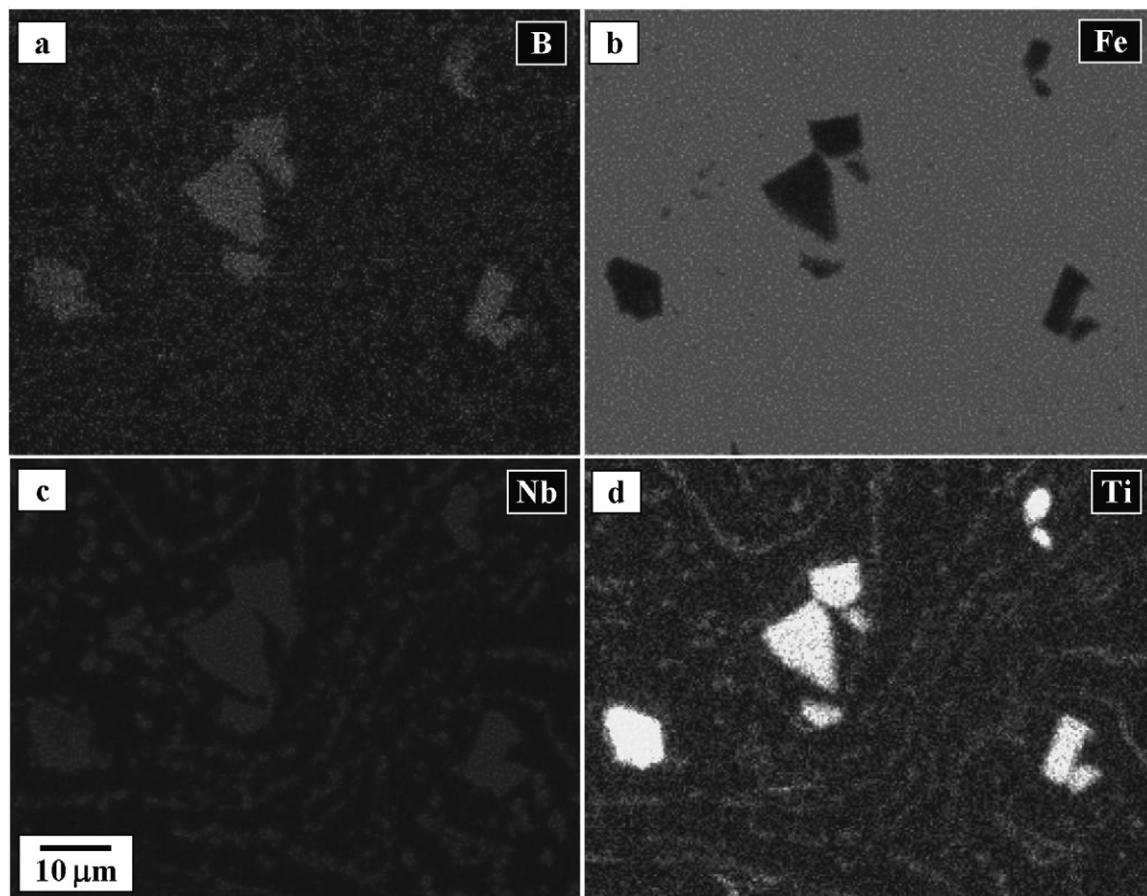


Fig. 8. X-ray dot mapping of Fig. 7 for B (a), Fe (b), Nb (c), Ti (d). Note that there is no Fe inside either the coarse or the fine Fe, Nb-containing borides.

$\Delta T_x = 38$  K was found in the thinnest (1.5–4 mm thick) regions of the spray formed deposit of alloy  $[(\text{Fe}_{0.6}\text{Co}_{0.4})_{0.75}\text{B}_{0.2}\text{Si}_{0.05}]_{96}\text{Nb}_4$ . The amorphous structure formation in this region was confirmed by TEM analysis, see Fig. 4. However, DSC traces of thicker parts of the deposit (6 and 16 mm) showed absence of exothermic reactions, an indication of fully crystalline structure. This result led us to suppose that an alloy that presents a BMG behaviour can result in an amorphous structure during deposition of first layers in contact with cold substrate by spray forming. This is a reasonable hypothesis considering the cooling rates prevailing during solidification of the deposit,  $10^1$ – $10^2$  K/s. However, when deposition progresses the solidified deposit becomes hotter due to the influence of latent heat released by the incoming droplets and the lower influence and heat extraction efficiency of the substrate in dissipating the heat, and can reach temperatures over  $T_x$ , if its thickness attains a critical value, leading to crystallization.

The rapid solidification process of melt spinning for the SF2 composition resulted in the formation of an amorphous ribbon with no clear  $T_g$  and with  $T_x$  of about 550 °C, as indicated by DSC analysis, showing a low glass forming ability for this composition (not a BMG former). This result was confirmed by XRD analysis of overspray powders of this composition, see Fig. 5, where the unsieved powder presented the formation of  $\text{Fe}_2\text{B}$  and  $\alpha$ -Fe phases, which were also the first phases to nucleate on a previous study with  $\text{Fe}_{66}\text{B}_{30}\text{Nb}_4$  alloy [4]. The peak broadening (mainly around 44°) and low counting (for the same  $\alpha$ -Fe peak) are evidence of nano-sized grains and/or some remaining amorphous phase or the metastable  $\text{Fe}_{23}\text{B}_6$  phase, as pointed out by Stoica et al. [3] and Imafuku et al. [6]. The presence of some amorphous phase was confirmed by an exothermic peak in DSC scans. Another exothermic crystallization

peak in DSC scans was observed for the SF1 experiment only in the size ranges up to 106–250  $\mu\text{m}$ . These results confirmed the low glass forming ability of these compositions allowing fully amorphous structure be obtained only by melt spinning (cooling rate of  $10^6$  K/s).

Comparing the results of the spray formed deposits of SF1 and SF2 experiments with the original composition  $\text{Fe}_{66}\text{B}_{30}\text{Nb}_4$ , reported earlier [4], which presented about 8.5% of amorphous phase in the thinnest regions of the deposits (<1 mm) proves, as expected, that the glass forming ability has been reduced with the titanium additions, as the deposits for both experiments showed fully crystalline phases. In addition, the results presented here for the alloys  $\text{Fe}_{63}\text{B}_{29}\text{Nb}_4\text{Ti}_4$  and  $\text{Fe}_{65}\text{B}_{30}\text{Nb}_4\text{Ti}_1$  demonstrate that an increase in the gas–metal ratio and/or the flight distance between the substrate and the atomizer nozzle or a decrease of the atomizing temperature, i.e., taking every possible steps to increase the cooling rates, did not suffice to prevent crystallization, if the alloy presents a low glass forming ability.

Approximately 70 and 100 ppm of nitrogen were found in SF1 and SF2 experiments, respectively, by thermal conductivity chemical analysis. This difference in the N content between SF1 and SF2 might be caused by the purge step with  $\text{N}_{2(g)}$  in the atomization chamber performed exclusively during SF2 experiment, which could increase the nitrogen available in solid solution in the deposit. As high purity elements were used, it is reasonable to suppose that a small amount of nitrogen was absorbed and produced nitrides such as  $\text{Fe}_3\text{N}$ , as all XRD scans from sampling of SF2 indicate in spite of the low counting of its peaks. The nitrogen preference for iron in detriment to boron may be caused by the higher iron content (and consequently higher activity) in these compositions. The

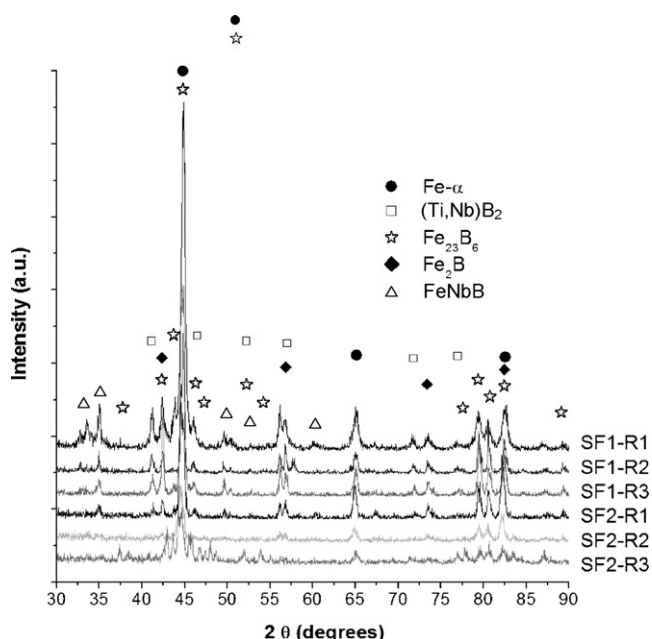


**Fig. 9.** XRD diffractograms for the deposits of SF1 (alloy with 4 at% Ti) and SF2 (alloy with 1 at% Ti) experiments, respectively, in positions R1 (center), R2 (middle) and R3 (boarder).

$\text{Fe}_3\text{N}$  could not be found by SEM/EDS, what, in addition to the low N content, makes reasonable to assume that this intermetallic has not affected significantly microhardness values obtained.

Aside its influence on the glass forming ability, the addition of titanium showed as well a significant modification of the  $\text{Fe}_{66}\text{B}_{30}\text{Nb}_4$  alloy's solidification. As pointed out by Imafuku et al. [6] and Stoica et al. [3] the alloy  $\text{Fe}_{66}\text{B}_{30}\text{Nb}_4$  solidifies under rapid solidification conditions by the formation of either an amorphous or an metastable  $(\text{Fe,Nb})_{23}\text{B}_6$  crystalline phase, which further might crystallize or decompose to  $\text{Fe}_2\text{B}$ ,  $\alpha\text{-Fe}$  and a  $\text{FeNbB}$  phase. Notwithstanding, the addition of titanium changed this sequence by forming, firstly, coarse titanium and niobium containing borides. According to the results of this work there are two possibilities, depending on the titanium content: for 4 at% Ti, experiment SF1,  $\text{TiB}_2$  and  $(\text{Ti,Nb})\text{B}_2$  are formed, and for 1 at% Ti, experiment SF2, only lower quantities of  $(\text{Ti,Nb})\text{B}_2$  is formed. Fig. 6 shows these borides at its upper right side for the former alloy that contains the higher titanium content, and Fig. 7 shows that only  $(\text{Ti,Nb})\text{B}_2$  is formed for the later alloy. These affirmations were based on X-ray dot mappings by using SEM/EDS analysis (see Fig. 8) and on XRD analysis, Fig. 9.  $\text{TiB}_2$  peaks were indexed using JCPDS files (file number 350741). The XRD patterns show the corresponding peaks at approximately  $35^\circ$  (1 0 0) and at approximately  $62^\circ$  (1 1 0). The formation of these coarse borides might have a strong influence on the solid state precipitation of a niobium, titanium boride as it will be described later.

The following solidification is similar for both alloys: proeutectic dendrites of  $\text{Fe}_2\text{B}$  intermetallic, whose arms are broken by the effect of the impacting droplets during deposit build-up, an eutectic of  $\alpha\text{-Fe}$ ,  $\text{Fe}_2\text{B}$ , and  $\text{FeNbB}$   $\tau$  phase according to XRD, see Fig. 9, and SEM/EDS analyses (Figs. 6–8). Metastable  $\text{Fe}_{23}\text{B}_6$  intermetallic phase was identified just for the thinnest region of SF2 deposit according to XRD analysis (identified as SF2-R3 pattern in Fig. 9). The microstructure of the SF2 deposit also presented precipitation in solid state of a niobium, titanium boride from the  $\alpha\text{-Fe}$  phase, see Fig. 7 (white particles) and a detail in Fig. 10 with higher magnification. This phase was identified by EDS dot mapping, see Fig. 8, where it is possible to observe that the Nb and Ti distributions are closely

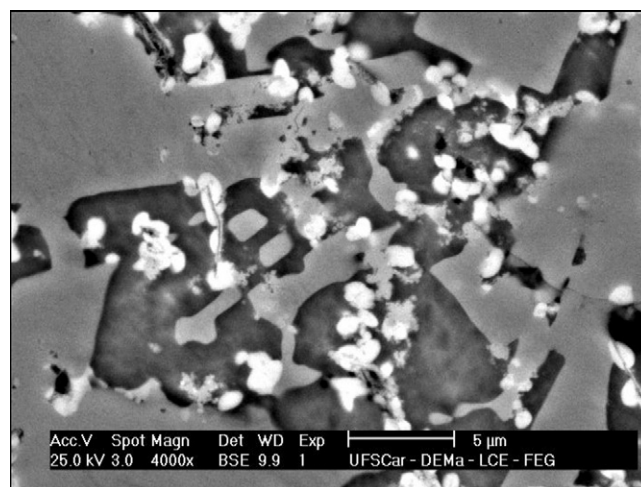


**Fig. 10.** Microstructure in the middle region of the SF2 deposit, higher magnification than in Fig. 7. Light particles are  $(\text{Nb,Ti})\text{B}$  precipitates, grey areas are proeutectic  $\text{Fe}_2\text{B}$  plates, and darker phases are  $\alpha\text{-Fe} + \text{Fe}_2\text{B} + \text{FeNbB}$ .

related to the presence of the white particles in Figs. 7 and 10. The presence of this precipitate showed a high influence on the hardness of the alloy  $\text{Fe}_{65}\text{B}_{30}\text{Nb}_4\text{Ti}_1$  and its presence is ascribed to a higher supersaturation of Nb and Ti in the  $\alpha\text{-Fe}$  for this composition in comparison with the alloy  $\text{Fe}_{63}\text{B}_{29}\text{Nb}_4\text{Ti}_4$ , where the higher titanium content consumed a higher quantity of Nb by forming the coarse primary borides observed in Fig. 6.

The metastable  $\text{Fe}_2\text{Nb}$  precipitation was not observed at all. Afonso et al. [7] also noted that this precipitation was suppressed in thinner regions of the deposit of  $\text{Fe}_{83}\text{Zr}_{3.5}\text{Nb}_{3.5}\text{B}_9\text{Cu}_1$ . Other intermetallic particles were found with variable Ti and Nb contents. The EDS analyses suggest small amount formation of  $(\text{Ti,Nb})\text{B}_2$  in rapidly solidified regions of the deposits, for example, close to substrate and in thinner sections. XRD analysis from the board regions of SF1 (0.7–2.5 mm) deposit has shown metastable borides:  $\text{Fe}_{23}\text{B}_6$ ,  $\text{Fe}_2\text{B}$  and some  $\text{FeB}$  which was also detected in SF2 XRD analyses in regions of similar thicknesses.

Hardness of the SF2 deposit attained values of  $839 \pm 85$  HV 30/20. Several exploratory tests showed an increase of Vickers hardness values with a decrease in the test load (kgf) applied; mainly, because indentations are more influenced by the large borides. In comparison with spray formed deposits of  $\text{Fe}_{66}\text{B}_{30}\text{Nb}_4$  produced with similar processing parameters [4], microhardness (measured at low loads in the range 0.2–5 kgf) has increased from  $804 \pm 77$  HV to  $943 \pm 103$  HV (SF2, alloy  $\text{Fe}_{65}\text{B}_{30}\text{Nb}_4\text{Ti}_1$ ) and from  $603$  HV to  $811 \pm 121$  HV (SF1, alloy  $\text{Fe}_{63}\text{B}_{29}\text{Nb}_4\text{Ti}_4$ ). Cracking was observed only for SF1 microindentation edges. Despite the higher hardness, the SF2 experiment has not presented cracks. Aside the influence of the niobium, titanium borides, which improved strongly the hardness of alloy  $\text{Fe}_{65}\text{B}_{30}\text{Nb}_4\text{Ti}_1$ , titanium may be responsible for the additional increase in Vickers hardness, probably by solid solution in SF1 (higher cooling rates) and precipitated as  $\text{Fe}_2(\text{Nb,Ti})$  in SF2 (lower cooling condition). This effect must, however, be studied more in detail.

According to the results of this work, amorfizable alloys  $\text{Fe}_{65}\text{B}_{30}\text{Nb}_4\text{Ti}_1$  and  $\text{Fe}_{63}\text{B}_{29}\text{Nb}_4\text{Ti}_4$  required cooling rates above  $10^5$ – $10^6$  K/s for amorphous phase formation. Therefore, the SF process was not able to produce amorphous deposits for these alloys even in the atomization step, where the highest cooling rates are imposed up to  $10^4$  K/s and most of the overspray particles hit the deposit in a partially amorphous or crystalline state. However, the process presents the possibility of producing these alloys with metastable phases and with very high hardness, at a very high production rate. On the other hand, by using an alloy with a higher glass

forming ability such as the alloy  $[(\text{Fe}_{0.6}\text{Co}_{0.4})_{0.75}\text{B}_{0.2}\text{Si}_{0.05}]_{96}\text{Nb}_4$  employed in this work, the process allows the production of amorphous phase in thicknesses similar to the ones delivered by the copper casting method, but by a considerable higher production rate. Notwithstanding, even employing an alloy with good glass forming ability, the production of amorphous and metastable phases through spray forming requires very high gas-to-metal ratios (G/M) to ensure deposition with a high volume fraction of rapidly and fully solidified amorphous particles. The choice of parameters for faster cooling may also represent a technological puzzle, since the process yield and the porosity of the deposit must be balanced with the amount or thickness of desired metastable material.

Finally, in order to enhance the possibility of producing fully, thicker amorphous deposits of BMG forming alloys, beyond the limits of copper casting, and to take advantage of the high production rates of the spray forming process, its cooling system must be adapted to meet the needs of the alloys.

#### 4. Conclusions

Spray formed deposit of the  $[(\text{Fe}_{0.6}\text{Co}_{0.4})_{0.75}\text{B}_{0.2}\text{Si}_{0.05}]_{96}\text{Nb}_4$  alloy resulted in fully amorphous structure for thicknesses up to 4 mm, confirming its high glass-forming ability. The  $\text{Fe}_{66}\text{Nb}_4\text{B}_{30}$  alloy modified with Ti presented fully crystalline deposits, although DSC analysis of melt spun ribbons suggested the possibility to promote amorphous phase formation. Ti additions to

the  $\text{Fe}_{66}\text{B}_{30}\text{Nb}_4$  alloy increased the hardness of spray formed materials by 17% and 35% for 4at% and 1at% Ti additions, respectively.

The successful production of amorphous deposits in BMG forming compositions by the spray forming process strongly depends on the glass forming ability (GFA) of the alloy in combination with process parameters that favor amorphization of the alloy.

#### Acknowledgements

The authors would like to thank Brazilian research financial agencies FAPESP (Fundação de Amparo a Pesquisa do Estado de São Paulo) and CAPES (Coordenação de Aperfeiçoamento de Pessoal de Nível Superior) for the financial support.

#### References

- [1] C.R.M. Afonso, C. Bolfarini, W.J. Botta, C.S. Kiminami, Mater. Sci. Eng. A 884 (2007) 449–451.
- [2] A. Inoue, B.L. Shen, C.T. Chang, Acta Mater. 52 (2004) 4093–4099.
- [3] M. Stoica, S. Kumar, S. Roth, S. Ram, J. Eckert, G. Vaughan, A.R. Yavari, J. Alloys Compd. 483 (2009) 632–637.
- [4] L.F. Bonavina, C. Bolfarini, W.J. Botta, E.R. D'Almeida, C.S. Kiminami, J. Alloys Compd. 495 (2010) 417–419.
- [5] E.J. Lavernia, Y. Wu, Spray Atomization and Deposition, John Wiley & Sons, Inc., New York, NY, 1996.
- [6] M. Imafuku, S. Sato, H. Koshiba, E. Matsubara, A. Inoue, Scripta Mater. 44 (2001) 2369–2372.
- [7] C.R.M. Afonso, C. Bolfarini, C.S. Kiminami, Mater. Sci. Eng. A 375–377 (2004) 571–576.